

## Localization and Identification of Faults in Power Line Network by TDR and Wavelet Transform

H. Harrat<sup>1</sup>, M. Chouki<sup>1</sup>, B. Nekhou<sup>1</sup>, S. Kaouche<sup>1</sup>, K. Kerroum<sup>2</sup> and K. El Khamlichi Drissi<sup>2</sup>

<sup>1</sup> LAMEL Laboratory, University of Jijel, BP 98 Ouled Aissa 18000 Jijel, Algeria

<sup>2</sup> LASMEA Laboratory, Blaise Pascal University, 24 Avenue des Landais, 63177 Aubière, France

Email: [haroun\\_harrat@hotmail.com](mailto:haroun_harrat@hotmail.com)

**Abstract:** In this paper, we present a procedure for the localization and the identification of a fault in power line network. For the localization of the faults the adopted method is the time domain reflectometry (TDR). The nature of the fault and its dominant frequency are deduced by using the traveling wave and wavelet transform. For this objective we consider the difference between the response of the line or network without and with fault when it's excited by impulse signal. This difference is treated by TDR and analyzed by wavelet transform in discrete in time-scale (DWT) and in continuous in time-frequency (CWT).

### Introduction

The quality of the electric power has become an important issue for electric utilities and their customers. The quality of the electric power is largely synonymous with the voltage quality and the continuity of the service. The general strategy to assure the continuity of the service of the power supply is based in the detection in real time of the fault affected the power network. Generally the defects appear less often in equipments (transformers) and most of the time in power line. For this reason it's essential to control the state of the power line. Classically, using the TDR technique; it's possible to localize the fault in line or cable.

Also, wavelet analysis is used in many areas of engineering and is specifically suited for examining non stationary phenomena. Since a few years, some works devoted to the analysis of signal records (voltages and currents) made on power networks by the wavelet technique are published in the literature [1]-[2]. Usually these works are to isolate in time frequency industrial of the frequencies caused by a fault. This allows us to locate in time the appearance of failure and possibly it's rang frequency.

In our work we propose a procedure for localization in space and in time by TDR and wavelet transform (DWT), and identification of the fault nature in power network by traveling wave. Also using wavelet transform (CWT) we deduce the dominant frequency in instant where appears the fault.

For this study we treat and deduce few information's in the power network response without and with fault. At first, it's essential to know the

response of the power network excited by impulse voltage. For this objective we use the formalism proposed by S. Kaouche [3]. The technique of the TDR and the response analysis by wavelet intervene subsequently.

The steps of the proposed procedure are described in the following:

- localization of a fault in space and in time in an electric network by TDR (time domain reflectometry) and discrete wavelet transform (DWT).
- identification of fault nature by travelling wave.
- the continuous wavelet transform (CWT) is applied to the difference of the responses (without and with fault) of the network in order to obtain a dominant frequency.

### Analysis of a Network Excited by a Localized Source

For the analysis of a network excited by a localized source, we use the topological formalism proposed by [3]. This formalism consists in translating the nature and the topology of the network in a matrix [A] making appear the lines and the set of the localized networks (nods of extremities and junctions). This procedure allows us to elaborate a system of linear equations:

$$[A] \times [X] = [B] \quad (1)$$

Where:

[X]: unknown vector (currents and nodes' voltage);

[B]: source vector.

The matrix [A] is composed by two submatrices, as follows:

$$[A] = \begin{bmatrix} [A_1] \\ [A_2] \end{bmatrix} \quad (2)$$

[A<sub>1</sub>]: is the submatrix deduced in temporal with recurrence equation in voltage [3].

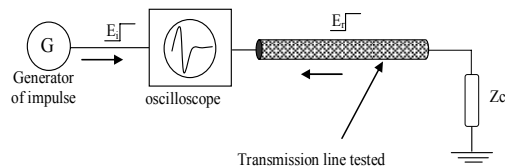
[A<sub>2</sub>]: is the submatrix deduced from the Kirchhoff's laws (KCL and KVL) for junctions (terminations' and interconnections' networks).

For an overhead line, it is important to take in consideration the frequency variation of the longitudinal impedance. The current recurrence equation takes into account this frequency dependence [3].

### Time Domain Reflectometry

The technique of time domain reflectometry (TDR) has been used by electrical engineers since the 1930s for testing the characteristics of transmission lines and diagnosing faults [4]. This technique is traditionally used to detect discontinuities in a transmission line. The TDR uses the echo effect, but, instead of operating under sinusoidal maintained signals, it uses echelons units or impulses, it results from a simple concept: when the energy transmitted in a meeting support in case of a change of impedance, a part of this energy is sent back to the source. The amount of energy reflected depends on the scale of the impedance changing.

In time domain reflectometry, an injected wave travels to the far end of the line, where it is reflected back, and circuitry at the source end of the line is used to receive this reflected voltage. The incident and reflected voltages are both seen on the line simultaneously, although their time domain signatures are generally separated in time because of the travel time delay down the line. The line impedance, termination, and length gives a unique temporal signature that can be used to determine the status of the line. Large changes in the line (open-end or short circuit) cause large reflections which are easy to measure, while small changes in the line (small defects, ..., etc) cause smaller reflections which are more difficult to detect. TDR electronics include a fast rise time pulse generator and fast voltage sampler, as well as a microprocessor to analyze the results. Typical rise times are about tens or hundreds of picoseconds, and samplers of similar order are available [5].



$E_i$  signal generator pulse injected into line  
 $E_r$  echo received from pulse (reflection)

**Figure 1:** Principle Diagram of the time domain reflectometry (TDR)

### Localization and Analyzing of Reflexion Points

In this work, a procedure is proposed to recognize the type of the fault in a line and to localize its position. In order to localize faults, it is very important to use very short pulses with fast rising edge. The distance  $x$  between a reflection point and the injection point is given by:

$$x = \frac{\tau \cdot v}{2} \tag{3}$$

Where  $v$  is the frequency-dependent propagation velocity of the signal into the line, and  $\tau$  is the sum of the time of the traveling wave from the source toward the damage and of the reflected wave from the damage toward the source.

### Wavelet Theory

A whole range of information: a voice, fingerprints, photographs, medical X-rays, of seismic waves can be transposed into this new language. These various studies use a new mathematical language whose alphabet consists of identical-oscillations “wavelet” wisely stretched or compressed. Often this wavelet transformation reduces the computation time, facilitates analysis, transmission and compression of information or its extraction from the “noise” surrounding.

For many signals, the low-frequency content provides the identity of the signal, while the high-frequency content gives flavour or nuance [6]. Wavelet analysis lets us capture these two different aspects of a signal, as approximation coefficients  $c_i(k)$  and detail coefficients  $d_i(k)$ . Approximations are the low frequency components of the signal; details are the high-frequency components. The approximations and details may be extracted using a discrete sampling or successive filtering technique. To extract the approximations and details as independent signals, we can pass the original signal  $x(t)$  through a pair of complementary low-pass and high-pass filters to get two signals. The low-pass filter  $h(n)$  yields the first level approximation coefficient  $c_i(k)$  and the high-pass filter  $g(n)$  yields the first level detail coefficient  $d_i(k)$ .

### The Wavelet Transform

A mother wavelet  $\psi$  is a basic function that we will translate and dilate the plan to cover time and frequency analysis of the signal [6].

The factors of translating  $u$  and scaling  $s$  are given by:

$$\Psi_{u,s}(t) = \frac{1}{\sqrt{s}} \psi\left(\frac{t-u}{s}\right) \tag{4}$$

The Wavelet Transform (WT) of a continuous signal  $x(t)$  is defined as:

$$Wf(u,s) = \frac{1}{\sqrt{s}} \int_{-\infty}^{+\infty} x(t) \psi\left(\frac{t-u}{s}\right) dt \tag{5}$$

### Discrete Wavelet Transform (DWT)

For many signals, the low-frequency content is the most important part; it gives the identity of the signal. The high-frequency content, on the other hand, imparts flavor or nuance [6]. Wavelet analysis lets us capture these two different aspects of a signal, as approximation

coefficients and detail coefficients. Approximations are the low frequency components of the signal; details are the high frequency components.

The wavelet transform has a digitally implementable counterpart, the Discrete Wavelet transform (DWT). The DWT is defined as [7]:

$$DWT[m, k] = \frac{1}{\sqrt{a_0^m}} \sum_n x[n] g\left[\frac{k - n.a_0^m}{a_0^m}\right] \quad (6)$$

Where  $g[n]$  is the mother wavelet, and the scaling and translation parameters  $u$  and  $s$  of (5) are functions of an integer parameter  $m$ ,  $u = a_0^m$  and  $s = n.a_0^m$ .

The result is geometric scaling, i.e.  $1, 1/u, 1/u^2, \dots$  and translation by  $0, n, 2n, \dots$

### The Continuous Wavelet Transform (CWT)

The continuous wavelet transform (CWT) is the sum over all time of the signal  $x(t)$  multiplied by a wavelet function  $\psi$  scaled and shifted :

$$C(\text{scale}, \text{position}) = \int_{-\infty}^{+\infty} x(t) \psi(\text{scale}, \text{position}, t) dt \quad (7)$$

### Implementation of Wavelets

Observation of the structure of equation (6) suggests an efficient filter bank implementation of the wavelet transform, as shown in Figure 2. With the variable swap of  $k$  for  $n$ , (6) can be rewritten:

$$DWT[m, n] = \frac{1}{\sqrt{a_0^m}} \sum_k x[k] g[a_0^{-m} n - k] \quad (8)$$

To show the similarity of (8) to the general equation for Finite Impulse Response (FIR) digital filters [7]:

$$y[n] = \frac{1}{c} \sum_k x[k] h[n - k] \quad (9)$$

This suggests that  $g[a_0^{-m} n - k]$  is the impulse response of a low-pass digital filter with transfer function  $G(w)$ . Then by selecting  $a_0 = 2$ , or  $a_0^{-m} = 1, 1/2, 1/4, 1/8, \dots$ , each dilation of  $g[n]$  effectively halves the bandwidth of  $G(w)$ .

The multi-stage filter bank shown in Figure 2 implements the DWT using the low-pass mother wavelet  $g[n]$  and its high-pass dual  $h[n]^2$ . Down sampling ( $2\downarrow$ ) at the output of the low-pass filter  $g[n]$  effectively scales the wavelet by two for the next stage.

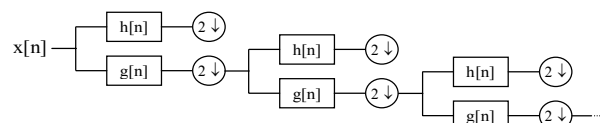


Figure 2: Multi-stage filter bank DWT implementation

### Application

The objective of our work is to characterize a fault on a power network. To do this, we use three different stages:

- 1) The first step is to locate the fault from the relationship (3).
- 2) The second stage allows us to identify its nature by calculating its impedance. For this second stage: (a)-we use the equations of recurrences for the deduction of voltage and current at the failure point, (b)-we deduct direct and inverse voltage at the failure point, (c)-we calculate the coefficient of reflection at the point of fault, (d)-we deduct the value of the impedance of the fault by using the located circuits' equations.
- 3) In the third stage we analyze the difference in responses with and without faults by wavelet transform.

In mathematical wavelet analysis we find a large number of wavelet mothers (Haar, Daubechies, Symlet, Coiflet, Meyer and Morlet,.....). In literature, depending on the signal 3D, 2D and 1D and domain of study preferences wavelet mothers are cited. It should be noted that generally the wavelets that are often used within the signal processing one-dimensional discrete are the Daubechies wavelets [6]. For our applications we use the four order Daubechies wavelet (noted db4), the order reflects the number of oscillations of the considered wavelet. A high order of the wavelet results in a lesser precision [6].

In our work of mathematical discrete analysis, we are interested to the effect of the convolution of the mother wavelet and its copies on the signal ( $s$ : the difference between healthy and noisy signals) while decomposing it at every frequency range into a detail signal of frequency in a signal of detail (designated by  $d$ ) plus a approximation (designated by  $a$ ) as follows:

$$s = \sum_i^n d_i + a_n \quad (10)$$

$d_i$  : designate the detail of the level  $i$  and  $a_n$  the last approximation.

Continuous analysis is to find a dominant pseudo-frequency in a frequency range, and the instant  $t$  of its appearance. The dominant frequency realizes the maximal norm of the coefficients vector of the wavelet in considered frequency rang, it is defined as follows:

$$|C| = \max_j \left( \sum_k |c_{jk}|^2 \right)^{1/2} \quad (11)$$

### Case of a Power Line

In first we consider a tri-phase horizontal power line of length 1km (figure 3) above soil of conductivity  $\sigma_s = 0.01 \text{ S/m}$ .

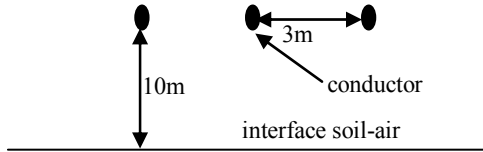


Figure 3: Horizontal power line

For characterize the fault we excite the power line by a generator of voltage  $V_s(t)$ .  $V_s(t)$  is the Gaussian type, with a spectral content that doesn't exceed the 10Mhz and whose mathematical expression is the following:

$$V_s(t) = e^{-\alpha(t-\beta.dt)^2}; \text{ Where } \alpha = (4/(\beta.dt))^2 \text{ and } \beta = 5.$$

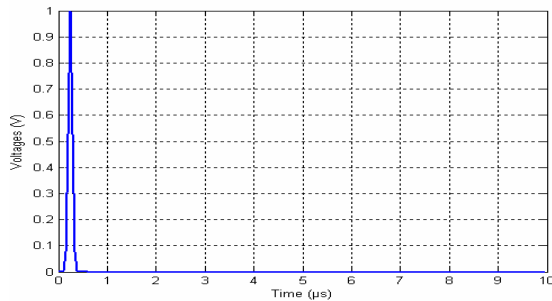


Figure 4: Voltage injected source

The line ending to her second extremity by loads of values roughly equal to the surge impedance.

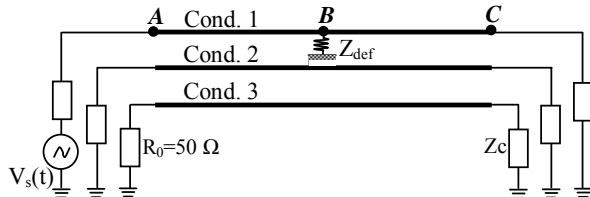


Figure 5: Line configuration

We considered a galvanic contact between the phase 1 and soil through a resistance the 10 Ω, situated to 500 m the beginning of the line.

According figure 6, we note the presence of two peaks reflecting negative reflections due to changes in impedance. The first reflection appears to the moment  $\tau_1 = 3.32\mu s$  that translates into a distance of approximately  $x = 496.34m$  the entry of phase 1 (point A). This reflection is due to an incident wave arriving from the point A and spreading to the fault (point B), located at 500m the entrance to the Phase 1, which is reflected back to the same point A, which is a wave that carries out an A-B-A journey. We note that the second reflection appears to the instant  $\tau_2 = 6.64 \mu s$  which is equivalent to a distance of about  $x = 992.68m$  the entry of Phase 1, it is due to mandatory second journey as short that occurs right after the first one, a wave that is a route that runs A-B-A-B-A, then it is a reflection due to contact the incident wave for a second time with the fault, this obstacle is already localized and it is at 500m

the point A. We note that this reflection can not be due to the ending of the second phase 1 because it is adapted (no reflection).

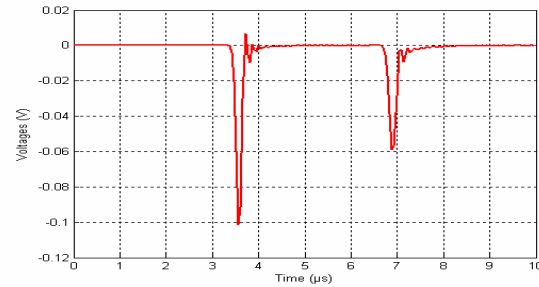


Figure 6: Signal difference between voltages with and without fault on the phase 1 to the point A

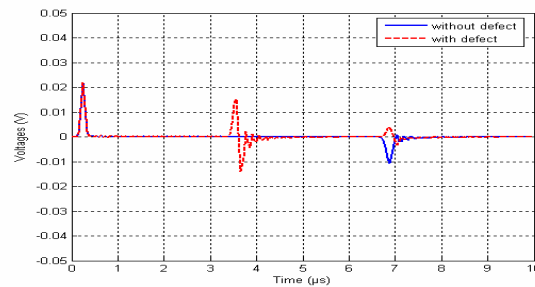


Figure 7: Variation of the voltage with and without fault at the entrance to Phase 2

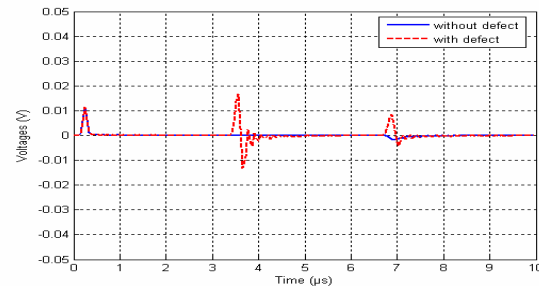


Figure 8: Variation of the voltage with and without fault at the entrance to Phase 3

The calculation of the coefficient of reflection and impedance localized to the point of fault, we can deduce a value approached to the impedance of fault  $Z_{fault}$  as:

$$Z_{fault} = -\frac{Z_c}{2} \left( \frac{\rho(x_{fault}) + 1}{\rho(x_{fault})} \right) \quad (12)$$

Where  $x_{fault}$  is the fault distance and  $\rho$  is the reflection coefficient in this point. In this example, the calculation of the reflection coefficient to the point of the fault drive to a value of -0.958, what is equivalent to impedance  $Z_{fault}$  that is equal 9.79Ω.

The analysis of the voltage at the entrance of the other two phases of the line (Figures 7 and 8), shows that the latter are hardly affected by the fault, we note very low voltage variations on phases 2 and 3. Indeed

the presence of the fault was demonstrated by the effect of electromagnetic coupling only (certainly the inductively coupled between the 3 power lines).

In order to complete our interpretation, we analyze the difference in responses without regard to the second reflection (figure 6) by wavelet (db4). The results will monitor are those that we get for a  $\Delta t = 4.88 \cdot 10^{-2} \mu s$  and a maximal frequency is  $\Delta f = 1/\Delta t = 20.84 \text{ MHz}$ .

In applying Shannon's theorem the frequency range will be in the meantime  $[0, 10.24] \text{ MHz}$ . For the discrete analysis, we will retain five details of decompositions: the 1<sup>st</sup> detail (d1) is definite by  $[5.12, 10.24] \text{ MHz}$ . the 2<sup>nd</sup> detail (d2) is definite by  $[2.56, 5.12] \text{ MHz}$ . the 3<sup>rd</sup> detail (d3) is definite by  $[1.28, 2.56] \text{ MHz}$ . the 4<sup>th</sup> detail (d4) is definite by  $[0.64, 1.28] \text{ MHz}$ . the 5<sup>th</sup> detail (d5) is definite by  $[0.32, 0.64] \text{ MHz}$ .

The signal approximation at level 5 is characterized by a frequency band  $[0, 0.32] \text{ MHz}$ .

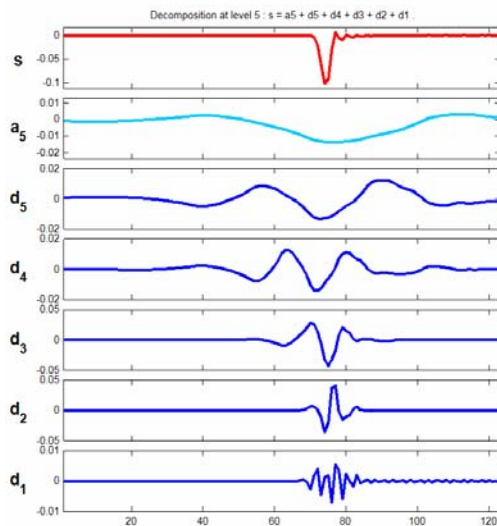


Figure 9: Decomposition, in five levels, of the signal difference at the entrance to the Phase 1

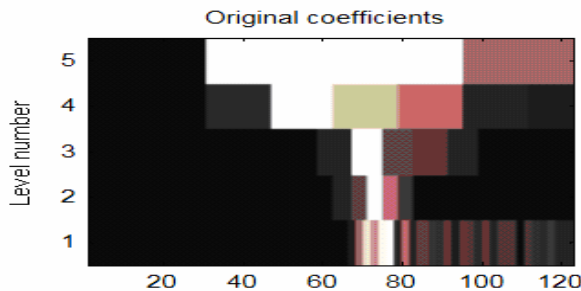


Figure 10: Spectrogram of the coefficients

In figure 9 we present the decomposition of the signal difference at the entrance of phase 1 of the line 1; this result shows an unexpected event in  $\tau_1 = 3.32 \mu s$  (which corresponds to the position 76 on the time scale), which represents the fault. The spectrogram of the

coefficients of wavelet (Figure 10) confirmed the presence of a dominant energy event in the same instant ( $\tau_1 = 3.32 \mu s$ ). We note also that the fault appears in the second detail (d2), and then it is well located on the third detail (d3) (figure 9). In that detail the frequency range is characterized by scale  $[1.28, 2.56] \text{ MHz}$ , which will certainly be the most dominant in terms of spectral density.

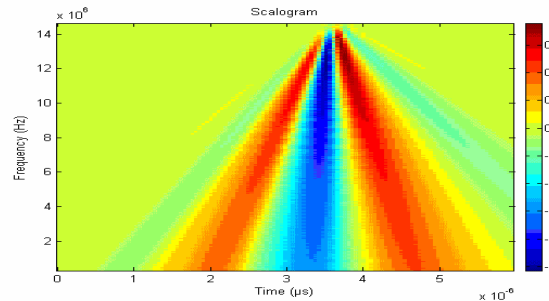


Figure 11: Scalogram of the coefficients of wavelet time-pseudo frequency

In order to complete our interpretation us proceed to an analysis in continuous of the coefficients of wavelet. Figure 11 introduced scalogram time coefficients in the frequency band  $[1.28, 2.56] \text{ MHz}$  for wavelet db4. The search of the optimum standard coefficients in the range frequency of level 3  $[1.28, 2.56] \text{ MHz}$ , leads us towards a pseudo-frequency dominant  $1.93 \text{ MHz}$ .

### Case of a Network with Double Fault

In our second application we consider 3 tri-phase power horizontal lines connected in Y (figure 12) with tri-phase bus bar; knowing that the lines lengths are  $L_1 = 500 \text{ m}$ ,  $L_2 = 1200 \text{ m}$ ,  $L_3 = 1000 \text{ m}$  and  $Z_c$  is surge impedance of the power lines. The lines are situated at 10m above the soil of conductivity  $\sigma_s = 0.01 \text{ S/m}$ .

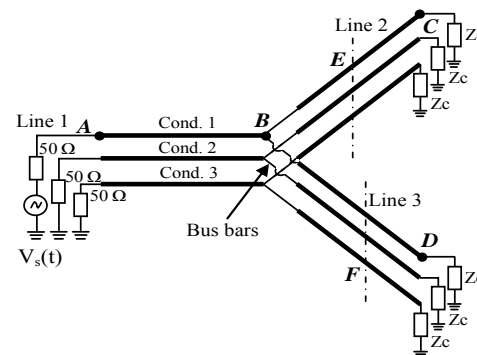
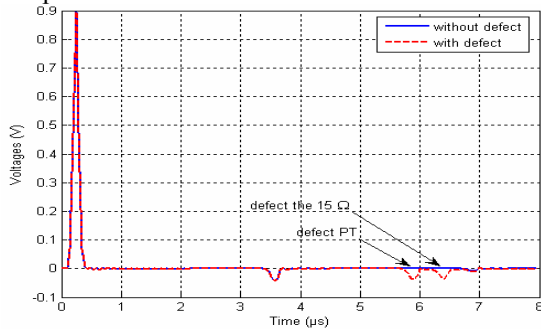


Figure 12: Power network in Y

We will use the same generator voltage  $V_s(t)$  Gaussian type (Figure 4) on the conductor 1 of line 1. We will analyze a double fault with a galvanic contact of  $15 \Omega$  between the phase 1 of the line 3 and the soil and situated in the F point to 430 m of the

interconnection (bus bar), and a short circuit between the phase 1 of the line 2 and soil (short circuit) situated to the point E to 350 m of the interconnection.



**Figure 13:** Variation of the voltage at the entrance to the line 1 (point A), with and without fault

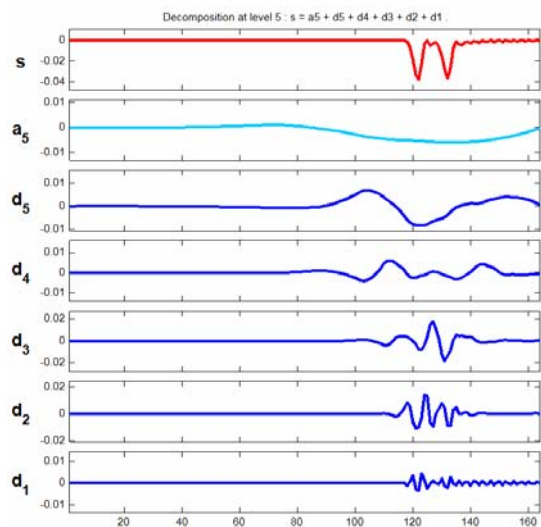


**Figure 14:** Decomposition of the signal difference at the entrance to the Phase 1 (on five levels of scale

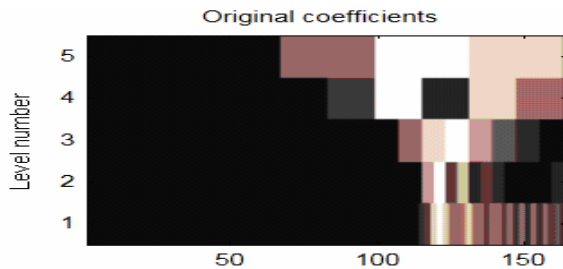


**Figure 15:** Spectrogram of the coefficients

The results in figure 13 put in evidence the presence of peaks that translates some reflections due to the changes of impedances. The first reflection in figure 13 appears at the instant  $\tau_1 = 3.32 \mu s$  which translates into a distance of about  $x = 496.34 m$  the entry of line 1 (point A) and characterize the position of the bus bar. The second reflection in figure 13 traduces the short circuit fault. In fact, the calculating of the reflection coefficient at the time of the second oscillation gives value of -1, what translates a short circuit.

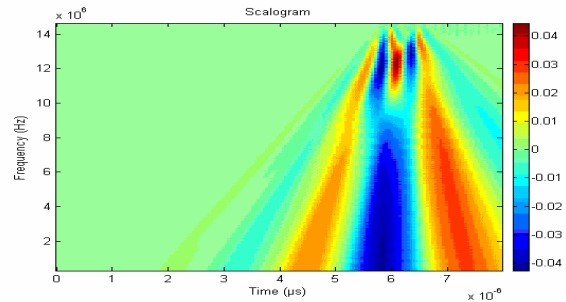


**Figure 16:** Scalogram wavelet time- frequency

To supplement our analysis we conduct an analysis of the continuous wavelet coefficients. The optimum of the norm of the coefficients respectively in the frequency scale 2 and 3 is realized where frequency value is 2.73 MHz for first fault (short circuit) and 1.7MHz for second (galvanic contact).

### Conclusion

The results we get for the various applications that we presented, showing that it is possible to make a full characterization of a fault on a line or a network simultaneously using the TDR and wavelet analysis. The procedure we propose to locate in space failure to short circuit using the TDR or discrete wavelet transform. The nature of the fault may be deduced in computing the impedance of fault using some concepts waves travelling and localized circuits. Finally it is also possible to deduce the dominant frequency at the time of fault by performing an analysis by continuous wavelet transform.

### References

- [1] C. Buccella, M. Feliziani and G. Manzi, "Accurate Detection of Low Enty Cable Faults by Wavelet transform," International Symposium on Electromagnetic Compatibility : EMC August 9-13 , 2004 Santa Clara, Cuba, pp. 936-941.
- [2] J. Chung, E. J. Powers, W. M. Grady and Sid C. Bhatt, "Electric Power Transient and Distrubance Classification Using Wavelet-Based Hidden Markov Models," 2000 IEEE Conference, pp. 3662-3665.
- [3] S. Kaouche, "Analyse de Défauts dans un Réseau de Lignes ou de Câbles", PHD Thesis, University of Jijel, Algeria, Jun 2007.
- [4] P. M. Hollywood, "TDR Level Measurement," Meas. Control, VOL. 31, N°. 6, pp 94-98, Dec. 1997.
- [5] C. Buccella, M. Feliziani and G. Manzi, "Detection and Localization of Defects in Shielded Cables by Time-Domain Measurements With UWB Pulse Injection and Clean Algorithm Postprocessing," IEEE Transactions on Electromagnetic Compatibility, VOL. 46, N°. 4, November 2004, pp. 597-605.
- [6] S. Mallat, A Wavelet Tour of Signal Processing. Academic Press, Second Edition, 1998.
- [7] D. C. Robertson, O. I. Camps, J. S. Mayer and W. B. Gish, "Wavelets and Electromagnetic Power System Transients," IEEE Transactions on Power Delivery, VOL. 11, N°. 2, April 1996, pp. 1050-1058.